Real-Time Blood Pressure Change Classification Using Enhanced PPG Signals and Convolutional Neural Networks

Devi Nurtiyasari[1,2], Abdurakhman[1,*] and Sumardi[1]

[1]*Department of Mathematics, Universitas Gadjah Mada, Sekip Utara, Yogyakarta, 55281, Daerah Istimewa Yogyakarta, Indonesia*

[2]*Mathematics Education Study Program, Sunan Kalijaga State Islamic University, Jl. Laksda Adisucipto, Yogyakarta, 55281, Daerah Istimewa Yogyakarta, Indonesia*

Abstract: Photoplethysmography (PPG) is widely used as a non-invasive and cost-effective technique for monitoring cardiovascular activity and assessing blood pressure (BP) variations. However, PPG signals are often affected by noise and motion artifacts, which can reduce signal reliability and negatively impact clinical interpretation and machine learning performance. This study proposes a signal enhancement and classification framework to improve the accuracy of BP change classification using PPG signals. The proposed approach enhances signal quality by reducing noise while preserving important physiological waveform characteristics, enabling more reliable feature extraction. The enhanced signals are then utilized as input to a Convolutional Neural Network (CNN) to learn discriminative temporal and morphological features associated with BP variations. Experimental results demonstrate that the proposed framework achieves a training accuracy of 96.66% and a validation accuracy of 95.31%, outperforming conventional preprocessing approaches such as hard and soft thresholding. These findings highlight the potential of integrating adaptive signal enhancement with deep learning techniques to improve the robustness and reliability of non-invasive BP monitoring systems. The proposed framework offers promising applications for real-time and clinically relevant cardiovascular monitoring.

Keywords: Photoplethysmography, Blood Pressure Classification, Enhanced Signals, Wavelet Denoising, Convolutional Neural Network, Deep Learning.

1. INTRODUCTION

Continuous and non-invasive monitoring of blood pressure (BP) plays a critical role in the early detection and prevention of cardiovascular diseases [1]. Conventional BP measurement techniques typically provide intermittent readings, which limit their ability to capture dynamic physiological variations that are essential for early risk assessment. These limitations highlight the need for reliable, real-time monitoring approaches that can support continuous cardiovascular evaluation in both clinical and wearable settings.

Photoplethysmography (PPG) has emerged as a promising alternative for non-invasive BP monitoring due to its simplicity, low cost, and ease of integration into wearable devices [2]. PPG signals reflect variations in blood volume within microvascular tissues and provide valuable insights into cardiovascular dynamics. However, the accurate interpretation of PPG signals remains challenging, as they are inherently nonlinear and non-stationary, and are often affected by noise and motion artifacts. These characteristics complicate the reliable classification of BP changes, particularly in real-time applications. In this study, PPG signals are utilized as the primary input modality due to their non-invasive nature and accessibility. To establish reliable reference labels, arterial blood pressure (ART) waveforms, obtained through invasive measurement, are employed to represent hemodynamic states such as dip, spike, and stable conditions. While ART signals provide accurate ground truth information, their invasive nature limits practical use. In contrast, PPG offers a scalable and patient-friendly alternative, enabling the development of predictive models for continuous BP monitoring without the need for invasive procedures.

Recent advances in deep learning have significantly improved the analysis of complex physiological signals. Convolutional Neural Networks (CNNs), in particular, have demonstrated strong capabilities in automatically extracting meaningful features from raw biomedical data. These models are well-suited for capturing both temporal and morphological characteristics of PPG signals, enabling improved classification of BP variations. The integration of deep learning techniques into cardiovascular monitoring systems has opened new opportunities for enhancing diagnostic accuracy and enabling real-time health assessment. Several studies have demonstrated the effectiveness of hybrid deep learning approaches in physiological signal analysis. Asad *et al*. [3] proposed a hybrid CNN-LSTM framework for real-time heart rate monitoring, achieving high predictive accuracy by combining spatial and

*Address correspondence to this author at the Department of Mathematics, Universitas Gadjah Mada, Sekip Utara, Yogyakarta, 55281, Daerah Istimewa Yogyakarta, Indonesia; E-mail: rachmanstat@ugm.ac.id

temporal feature extraction. Similarly, Batool [4] explored the use of deep learning for BP-related signal analysis, while Oleiwi *et al*. [5] employed CNN architecture for arrhythmia classification in imbalanced datasets. These studies highlight the growing potential of deep learning models in capturing complex patterns in biomedical signals and improving real-time monitoring capabilities.

Motivated by these developments, this study proposes a deep learning-based framework for real-time BP change classification using continuous PPG signals. The proposed approach focuses on enhancing signal quality and leveraging CNN architecture to extract discriminative features associated with BP variations. By improving both signal representation and feature learning, the framework aims to increase the robustness and reliability of BP classification in dynamic and real-world conditions. The contributions of this study lie in developing a clinically relevant and computationally efficient framework for non-invasive BP monitoring. By combining adaptive signal enhancement with deep learning classification, this work contributes to advancing real-time cardiovascular monitoring systems that are suitable for wearable and remote healthcare applications.

The remainder of this paper is organized as follows. Section 2 reviews related work and theoretical background. Section 3 presents the proposed methodology and model architecture. Section 4 discusses the experimental results and analysis. Finally, Section 5 concludes the study and outlines future research directions.

2. RELATED WORKS

The foundation of modern signal denoising techniques can be traced back to the work of Donoho and Johnstone [6], who introduced wavelet shrinkage as an adaptive method for estimating unknown smoothness in noisy data. This approach enables selective noise suppression while preserving essential signal features, providing a mathematically grounded framework for multiresolution signal analysis. Subsequent developments, including soft thresholding techniques [7], further improved the ability to remove high-frequency noise components without significantly distorting relevant signal structures. Later, Donoho and Johnstone [8] extended these concepts through minimax estimation, establishing statistical optimality in denoising under Gaussian noise conditions. These foundational studies have played a critical role in shaping modern signal preprocessing techniques widely used in biomedical applications, including the analysis of photoplethysmography (PPG) signals.

In parallel, the rapid advancement of deep learning has significantly transformed the analysis of biomedical and physiological signals. Convolutional Neural Networks (CNNs) have demonstrated strong capabilities in feature extraction and classification tasks, particularly in complex and high-dimensional data environments. Alzubaidi *et al*. [9] provided a comprehensive overview of CNN architectures across various domains, while Alqudah and Moussavi [10] highlighted their effectiveness in biomedical signal processing and clinical decision support systems. Similarly, Mienye *et al*. [11] discussed the application of CNNs in medical data interpretation, and Lee *et al*. [12] emphasized the optimization of CNN architectures for improved computational efficiency. Collectively, these studies demonstrate the robustness and adaptability of CNN models in extracting meaningful representations from physiological signals such as PPG.

Recent studies have further explored the integration of machine learning and deep learning techniques for non-invasive BP estimation and cardiovascular monitoring. Chen *et al*. [13] proposed a continuous BP estimation framework based on machine learning, demonstrating the potential of data-driven approaches in cardiovascular risk assessment. In a related context, Oleiwi *et al*. [5] introduced a hybrid CNN-GRU model for arrhythmia prediction using electrocardiogram (ECG) data, effectively capturing both spatial and temporal dependencies in physiological signals. Additionally, Batool [4] developed a deep learning-based architecture integrated with 5G infrastructure for real-time remote patient monitoring, illustrating how continuous physiological data analysis can enhance telemedicine systems. Furthermore, Asad *et al*. [3] proposed hybrid architectures combining convolutional and recurrent networks for predictive healthcare applications, emphasizing the importance of multi-scale feature extraction and temporal modeling.

More recently, Hong *et al*. [14] focused on real-time classification of blood pressure changes using PPG signals and deep learning techniques. Their findings demonstrate that deep neural networks are capable of capturing subtle variations in PPG waveforms associated with BP fluctuations. This highlights the growing potential of PPG-based approaches in enabling continuous, cuffless, and non-invasive BP monitoring

systems, which are essential for next-generation cardiovascular healthcare applications.

Despite these advancements, several challenges remain in developing robust and reliable BP monitoring systems. Physiological signals such as PPG are inherently nonlinear, non-stationary, and highly sensitive to noise and motion artifacts, which can significantly affect model performance. Moreover, achieving a balance between signal quality enhancement, computational efficiency, and accurate feature extraction remains an ongoing challenge in real-time applications. Therefore, there is a need for integrated frameworks that can effectively enhance signal quality while leveraging deep learning techniques to improve classification performance in dynamic and real-world environments.

In this context, this study focuses on developing a deep learning framework for real-time BP change classification using continuous PPG signals. By combining effective signal enhancement strategies with CNN feature learning, the proposed approach aims to improve the robustness and reliability of non-invasive cardiovascular monitoring systems.

3. METHODOLOGY FOR REAL-TIME BP DYNAMICS CLASSIFICATION

3.1. Data Description

The dataset employed in this study was derived from VitalDB, a high-fidelity multi-parameter vital signs database developed by Lee and colleagues at Seoul National University Hospital. VitalDB was designed to facilitate advanced research in perioperative monitoring by providing synchronized intraoperative waveform and numeric data recorded from more than six thousand surgical cases. The dataset includes high-resolution physiological signals sampled at 500 Hz, along with comprehensive perioperative parameters and clinical metadata [15, 16].

In this study, only two physiological waveform tracks were utilized from the VitalDB dataset, namely SNUADC PLETH (PPG) and SNUADC ART (ART). These two channels were selected because they represent fundamental hemodynamic signals commonly used in clinical monitoring and physiological modeling. The PLETH signal reflects peripheral blood volume changes measured optically, while the ART signal provides a direct measurement of arterial BP through invasive monitoring. The combination of these two signals enables a detailed analysis of cardiovascular dynamics and serves as a robust basis for evaluating signal processing and predictive modeling approaches.

The PLETH signal, hereafter referred to as PPG, is a non-invasive optical signal that reflects blood volume changes in peripheral tissue. In contrast, the ART signal represents invasive arterial BP measurements, providing a direct reference for hemodynamic fluctuations. In this study, the PPG waveform was used as the input signal, while the ART waveform served as the reference signal for generating the classification labels corresponding to three BP states: dip, spike, and stable. These classes were defined based on arterial pressure variations exceeding a threshold of 5 mmHg, following the classification framework proposed by Hong *et al*. [14] in their study on real-time BP change detection using PPG and deep learning.

From the entire VitalDB dataset, a total of 1,772 surgical cases were selected based on the availability of both the SNUADC PLETH (PPG) and SNUADC ART tracks. This filtering process ensured that only cases containing synchronized recordings of the non-invasive PPG and invasive arterial pressure signals were included for analysis. The selected subset thus provides sufficient temporal alignment and signal quality for evaluating the relationship between peripheral PPG dynamics and corresponding arterial BP variations. The characteristics of the SNUADC PLETH (PPG) and SNUADC ART tracks used in this study are detailed in Table **1**.

3.2. Data Preparation

This stage focuses on organizing and preparing the raw PPG and ART signals from the VitalDB dataset for further analysis. All data processing and visualization were performed using the Python programming language, supported by libraries such as vitaldb, numpy, pandas, and matplotlib. The Vital() function from the official VitalDB Python library was used to load waveform data for each patient.

Table **2** shows a sample of synchronized PPG and ART signals extracted from the VitalDB dataset. The columns represent the raw PPG amplitude, invasive ART BP, converted PPG voltage, and normalized PPG values. Each case file initially comprised approximately 1,994 samples. The resulting dataset consisted of 1,772 patient cases, each containing synchronized and downsampled waveform segments that were

Table 1: Characteristics of the PPG and ART Tracks Used in this Study

Aspect	PPG	ART
Signal type	Optical, non-invasive PPG measuring peripheral blood volume changes.	Invasive arterial BP waveform obtained from a catheter.
Clinical context	Recorded continuously during anesthesia and surgery via pulse oximetry modules.	Used during surgeries requiring invasive BP monitoring.
Sampling rate	62.5-500 Hz depending on device.	62.5-500 Hz, synchronized with PPG.
Measurement method	Non-invasive optical detection (infrared + red light).	Direct invasive pressure transduction via arterial catheter.
Use in this study	Used as *input* signal for classification.	Used as *reference* for generating dip/spike/stable labels.

Table 2: Partial Representation of the PPG and ART Dataset Showing Raw, Converted, and Normalized Signal Values

PPG	ART	Time	PPG_Volt	PPG_Norm
40.714203	102.77298	0.000	0.814284	0.407142
40.714203	101.785492	0.008	0.814284	0.407142
40.319229	99.810577	0.016	0.806385	0.403192
40.319229	98.823151	0.024	0.806385	0.403192
40.319229	97.835663	0.032	0.806385	0.403192
39.924240	95.860748	0.040	0.798485	0.399242
40.319229	95.860748	0.048	0.806385	0.403192
39.924240	94.873322	0.056	0.798485	0.399242
44.664032	94.873322	0.064	0.893281	0.446640
44.664032	99.810577	0.072	0.893281	0.446640

subsequently employed for feature extraction and model development.

To illustrate the preprocessing of PPG signals, Figure **1** presents a 10-second segment extracted from one patient case. The left panel shows the original PPG waveform, while the right panel depicts the normalized PPG signal after amplitude conversion. The normalization process ensures consistent signal scaling across different patients, facilitating fair comparison and improving the reliability of model training.

3.3. BP Feature Extraction from ART Waveform

To characterize blood pressure dynamics in a clinically meaningful manner, the ART waveform was segmented and analyzed to extract key hemodynamic parameters, namely *systolic blood pressure (SBP)* and

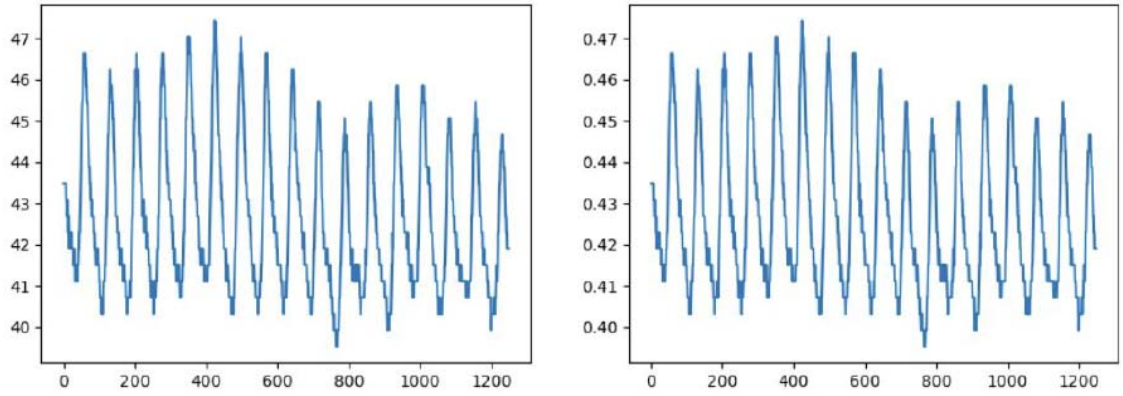

Figure 1: A 10-second PPG segment and its normalized waveform extracted from one patient record.

diastolic blood pressure (DBP). These parameters provide essential information regarding cardiovascular function and are widely used in clinical assessment and monitoring.

A copy of the synchronized PPG and ART dataset (vital.df_ppg_art) was created to preserve the original data integrity. The raw PPG signal was extracted and divided into fixed-length segments of 10 seconds, based on a sampling frequency of 125 Hz (resulting in 1,250 samples per segment). Each segment was validated using a predefined signal-quality function (is_ppg_valid()) to ensure that only physiologically meaningful portions (i.e., without sensor detachment or excessive noise) were retained for further analysis.

For every valid 10-second segment, the corresponding ART waveform was processed to detect systolic and diastolic peaks using the find_peaks() function from the SciPy library. Systolic peaks were identified as local maxima of the ART signal, while diastolic troughs were detected as local minima by applying the same function to the inverted waveform (-art). A minimum peak distance of 0.4 s was enforced to prevent the detection of spurious peaks within a single cardiac cycle.

Once the peaks and troughs were obtained, the average systolic (SBP) and diastolic (DBP) pressures were computed across all detected cycles within each segment. The mean blood pressure (MBP), which represents the average arterial pressure during a single cardiac cycle, was then derived using the standard hemodynamic relation:

$$MBP = \frac{SBP + 2 \times DBP}{3} \tag{1}$$

To capture temporal variations in cardiovascular dynamics, the change in MBP between consecutive segments (ΔMBP) was calculated. Based on this variation, a categorical variable BP_Class was defined to represent clinically relevant BP trends:

- **spike**: when $\Delta MBP > 5\ mmHg$,
- **dip**: when $\Delta MBP < -5\ mmHg$,
- **stable**: otherwise.

The extracted SBP, DBP, and MBP values were stored in a structured DataFrame (df_labels) for subsequent analysis and model training. Figure **2** illustrates one representative 10-second ART segment from the dataset, along with the corresponding systolic and diastolic pressure levels computed from the detected waveform peaks.

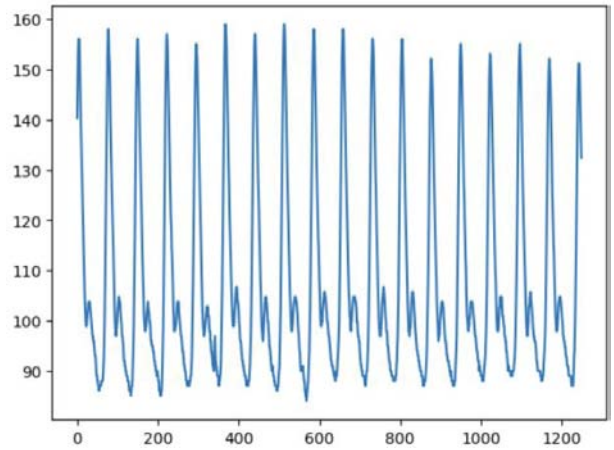

Figure 2: A 10-second ART pressure waveform showing systolic (SBP = 155.821 mmHg) and diastolic (DBP = 86.799 mmHg) levels extracted from the second segment of the dataset.

3.4. Signal Enhancement Using Wavelet-Based Denoising

Physiological signals such as photoplethysmogram (PPG) are frequently affected by motion artifacts and high-frequency noise arising from subject movement and measurement devices. These disturbances may degrade signal quality and, consequently, affect the reliability of downstream analysis, particularly in clinical contexts where accurate interpretation of waveform morphology is required. To mitigate these effects, a wavelet-based denoising approach is employed to improve signal quality prior to classification.

Wavelet denoising provides a time-frequency representation that enables selective attenuation of noise while preserving relevant physiological characteristics of the signal [6, 17]. This property is particularly suitable for PPG signals, which exhibit nonlinear and non-stationary behavior.

3.4.1. Mathematical Formulation

Let $x(t)$ denote the observed PPG signal, which consists of a true physiological component $s(t)$ and additive noise $n(t)$:

$$x(t) = s(t) + n(t) \tag{2}$$

The signal is decomposed using the Discrete Wavelet Transform (DWT) into approximation and detail coefficients:

$$W_{j,k} = \langle x(t), \psi_{j,k}(t) \rangle \tag{3}$$

where $\psi_{j,k}(t)$ denotes the wavelet basis function at scale j and position k. The decomposition process can be expressed recursively as:

$$A_j(t) = \sum_k h(k) A_{j-1}(2t-k) \tag{4}$$

$$D_j(t) = \sum_k g(k) A_{j-1}(2t-k) \tag{5}$$

here $h(k)$ and $g(k)$ represent low-pass and high-pass filters, respectively.

3.4.2. Thresholding Strategies for Signal Enhancement

The denoising framework in this work follows the multi-resolution analysis (MRA) principles introduced by Mallat (1999) and the wavelet thresholding approach proposed by Donoho (1995). A similar baseline framework has been applied in stock price prediction [19]. In this study, an enhanced thresholding strategy is introduced to accommodate local signal characteristics. The denoising process consists of three main stages:

1. Decomposition: The PPG signal is decomposed into multiple resolution levels to separate low-frequency trends from high-frequency noise.

2. Thresholding: A threshold is applied to suppress coefficients dominated by noise. The universal threshold [6] is defined as:

$$T = \sigma\sqrt{2\ln N} \tag{6}$$

where σ represents the noise standard deviation and N is the signal length. In this study, σ is estimated using the median absolute deviation (MAD) of the finest-scale coefficients to provide a robust estimate of noise variance.

Three thresholding strategies are considered:

Hard Thresholding removes coefficients below the threshold:

$$\hat{W}_{j,k} = \begin{cases} W_{j,k}, & |W_{j,k}| \geq T \\ 0, & |W_{j,k}| < T \end{cases} \tag{7}$$

Soft Thresholding shrinks coefficients toward zero:

$$\hat{W}_{j,k} = sign(W_{j,k}) \cdot \max(|W_{j,k}| - T, 0) \tag{8}$$

Enhanced Thresholding adopts a data-adaptive strategy in which the threshold is adjusted according to local signal characteristics across different segments of the waveform. This adaptive behavior facilitates a balance between noise suppression and feature preservation, which is particularly relevant for non-stationary physiological signals such as PPG. A more detailed formulation of this approach is presented in a separate study. In this work, the enhanced strategy is employed as a preprocessing step to improve the stability and quality of the input signal for classification. Compared to fixed global thresholding, this approach better accommodates variations in signal amplitude and structure, thereby supporting the preservation of important morphological features such as systolic peaks and dicrotic notches.

3. Reconstruction: The denoised signal is reconstructed using the inverse wavelet transform:

$$\hat{s}(t) = \sum_{j,k} \hat{W}_{j,k} \psi_{j,k}(t) \tag{9}$$

The resulting enhanced PPG signal preserves essential morphological characteristics required for cardiovascular analysis. This preprocessing step contributes to improving the stability of the signal representation and supports more reliable performance in subsequent classification tasks.

3.4.3. Simulation of Wavelet-Based PPG Signal Denoising

To illustrate the effectiveness of the denoising process, a simulated PPG segment was used to demonstrate how signal reconstruction behaves under noise contamination.

A short representative segment of the original PPG waveform was selected to ensure that waveform morphology and reconstruction details remain visually interpretable within a single figure. Quantitative evaluation of reconstruction quality was performed using the signal-to-noise ratio (SNR), defined as

$$SNR = 10\log_{10}\left(\frac{\sum_t x(t)^2}{\sum_t (x(t)-\hat{x}(t))^2}\right), \tag{10}$$

where $x(t)$ denotes the reference signal and $\hat{x}(t)$ represents the reconstructed (denoised) signal. Higher SNR values indicate improved signal quality and reduced residual noise.

Figure **3** presents the selected PPG segment alongside reconstructed signals obtained using standard wavelet thresholding strategies. The corresponding SNR values demonstrate that the

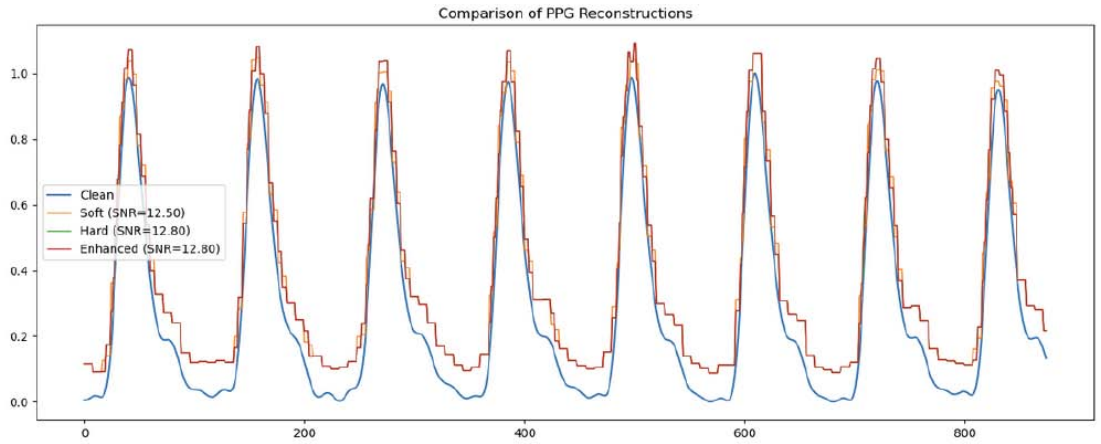

Figure 3: Representative PPG segment and reconstructed signals using different thresholding strategies. Legend indicates the reconstruction method and the corresponding SNR (dB).

denoising process improves signal quality while preserving the essential morphological characteristics of the PPG waveform.

Although the numerical differences between reconstruction strategies are relatively small, the denoised signals consistently maintain key physiological features such as waveform peaks and temporal structure. This indicates that wavelet-based denoising provides an effective balance between noise suppression and preservation of clinically relevant signal information.

3.5. Classification Using Convolutional Neural Networks (CNN)

Following the denoising stage, the denoised PPG signals were utilized as inputs for a deep learning model based on the CNN architecture. Deep learning models are particularly well-suited to handle time-series data produced by wearable sensors [18]. CNN, in particular, are effective for physiological signal analysis because they can automatically extract hierarchical spatial-temporal features without the need for manual feature engineering. In this study, the denoised PPG signals obtained from the wavelet thresholding process were utilized to train a CNN for BP trend classification (*spike*, *dip*, and *stable*). The research architecture, including the processes of data filtering, data preparation, preprocessing using enhanced signals, and classification, is illustrated in Figure **4**.

3.5.1. Input Representation

Each PPG segment of 10 seconds (1,250 samples at 125 Hz) was used as a single input instance. Before feeding into the CNN, signals were normalized to the range [0, 1] to ensure numerical stability during training. This preprocessing step ensures consistent feature scaling across different patients and recording sessions.

3.5.2. Network Architecture

The CNN architecture consisted of the following layers:

1. **Input Layer:** Accepts a one-dimensional PPG segment as input.

2. **Convolutional Layers:** Two convolutional layers with kernel sizes of 3 and 5 were employed to capture both fine-grained and broader waveform features. Each convolutional layer was followed by the ReLU activation function.

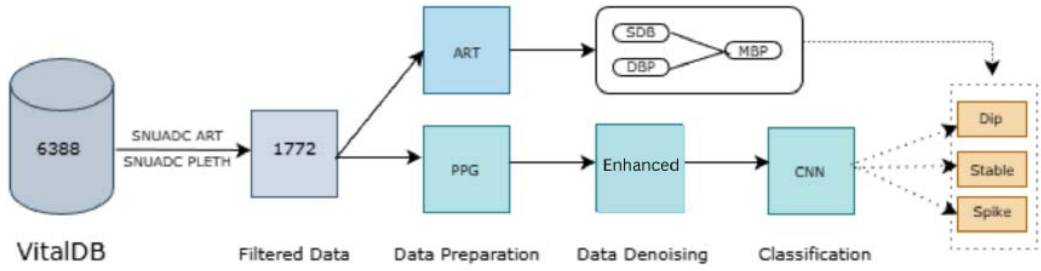

Figure 4: Research Architecture.

3. **Pooling Layer:** A max-pooling operation was applied to reduce spatial dimensionality and improve translation invariance.

4. **Fully Connected Layers:** Two dense layers aggregated the extracted features and performed non-linear transformations.

5. **Output Layer:** A softmax layer with three output neurons corresponding to the classes *spike*, *dip*, and *stable*.

3.5.3. Training and Optimization

The CNN model was trained using the Adam optimizer, which is widely adopted in deep learning due to its ability to adaptively adjust learning rates for each parameter, thereby improving convergence stability in complex optimization landscapes. The training process aimed to minimize the categorical cross-entropy loss function, defined as:

$$\mathcal{L} = -\sum_{c=1}^{C} y_c \log(\hat{y}_c), \tag{11}$$

where C denotes the number of classes, y_c represents the ground truth label, and $\hat{y}_c$ is the predicted probability for class c. This loss function is particularly suitable for multi-class classification tasks, as it quantifies the divergence between the predicted probability distribution and the true class distribution.

The optimization process was carried out iteratively using mini-batch gradient descent, where model parameters were updated based on the computed gradients of the loss function with respect to the network weights. The Adam optimizer combines the advantages of both momentum-based and adaptive learning rate methods, allowing efficient handling of non-stationary and noisy gradients commonly encountered in physiological signal data such as PPG.

To ensure stable convergence and avoid issues such as overfitting or vanishing gradients, key hyperparameters including the learning rate and batch size were determined empirically. This tuning process involved monitoring the training dynamics and validation performance to achieve a balance between convergence speed and generalization capability. The selected configuration enabled the model to effectively learn discriminative temporal and morphological features relevant to BP classification while maintaining robustness across varying signal conditions.

3.6. Evaluation

Model performance was evaluated using standard multi-class classification metrics, including accuracy, precision, recall, and F1-score. These metrics provide a comprehensive assessment of both overall performance and class-wise discrimination ability. The confusion matrix was employed to visualize classification results across the three classes, namely *spike*, *dip*, and *stable*, and to identify potential misclassification patterns among these physiological states.

To ensure robustness and generalization across different patient profiles, cross-validation was conducted by partitioning the dataset into multiple folds and evaluating model performance across these subsets.

The evaluation metrics are defined as follows.

Overall accuracy is computed as:

$$Accuracy = \frac{\sum_{i=1}^{C} TP_i}{N} \tag{12}$$

where C denotes the number of classes, TP_i represents the correctly classified samples for class i, and N is the total number of samples.

For each class i, precision and recall are defined as:

$$Precision_i = \frac{TP_i}{TP_i + FP_i} \tag{13}$$

$$Recall_i = \frac{TP_i}{TP_i + FN_i} \tag{14}$$

The F1-score for each class is computed as:

$$F1_i = 2 \times \frac{Precision_i \times Recall_i}{Precision_i + Recall_i} \tag{15}$$

To obtain a single performance measure, macro-averaged metrics are used:

$$Precision_{macro} = \frac{1}{C} \sum_{i=1}^{C} Precision_i \tag{16}$$

$$Precision_{macro} = \frac{1}{C} \sum_{i=1}^{C} Precision_i \tag{17}$$

$$F1_{macro} = \frac{1}{C} \sum_{i=1}^{C} F1_i \tag{18}$$

4. RESULTS AND DISCUSSION

Three thresholding techniques, the enhanced approach, Hard Thresholding, and Soft Thresholding, were applied in the preprocessing stage to evaluate the effects on the training and validation performance of the models. Each configuration was trained and evaluated over 300 epochs to ensure convergence and model stability. As illustrated in Figure **5**, all thresholding methods demonstrated a steady increase in training accuracy throughout the 300 training epochs, indicating stable learning behavior across the three approaches. Figure **6** provides a combined comparative plot that allows their performance trends to be examined within a single visualization. Because each method follows its own convergence pattern, the optimal epoch differs across techniques. The best model for each method was identified by selecting the checkpoint that achieved the highest accuracy within the validation and testing window.

The three thresholding strategies produced comparable performance. However, the enhanced approach achieved higher peak accuracy, reaching 96.660% at epoch 299, compared with Hard Thresholding at 96.630% (epoch 286) and Soft Thresholding at 96.280% (epoch 300). Although the differences are modest, this result indicates that the enhanced approach offers a small but consistent advantage in accuracy while maintaining stable convergence behavior. Similarly, the validation accuracy results shown in Figure **6** reveal a consistent performance trend, showing that the models maintained stable accuracy on unseen data. The enhanced

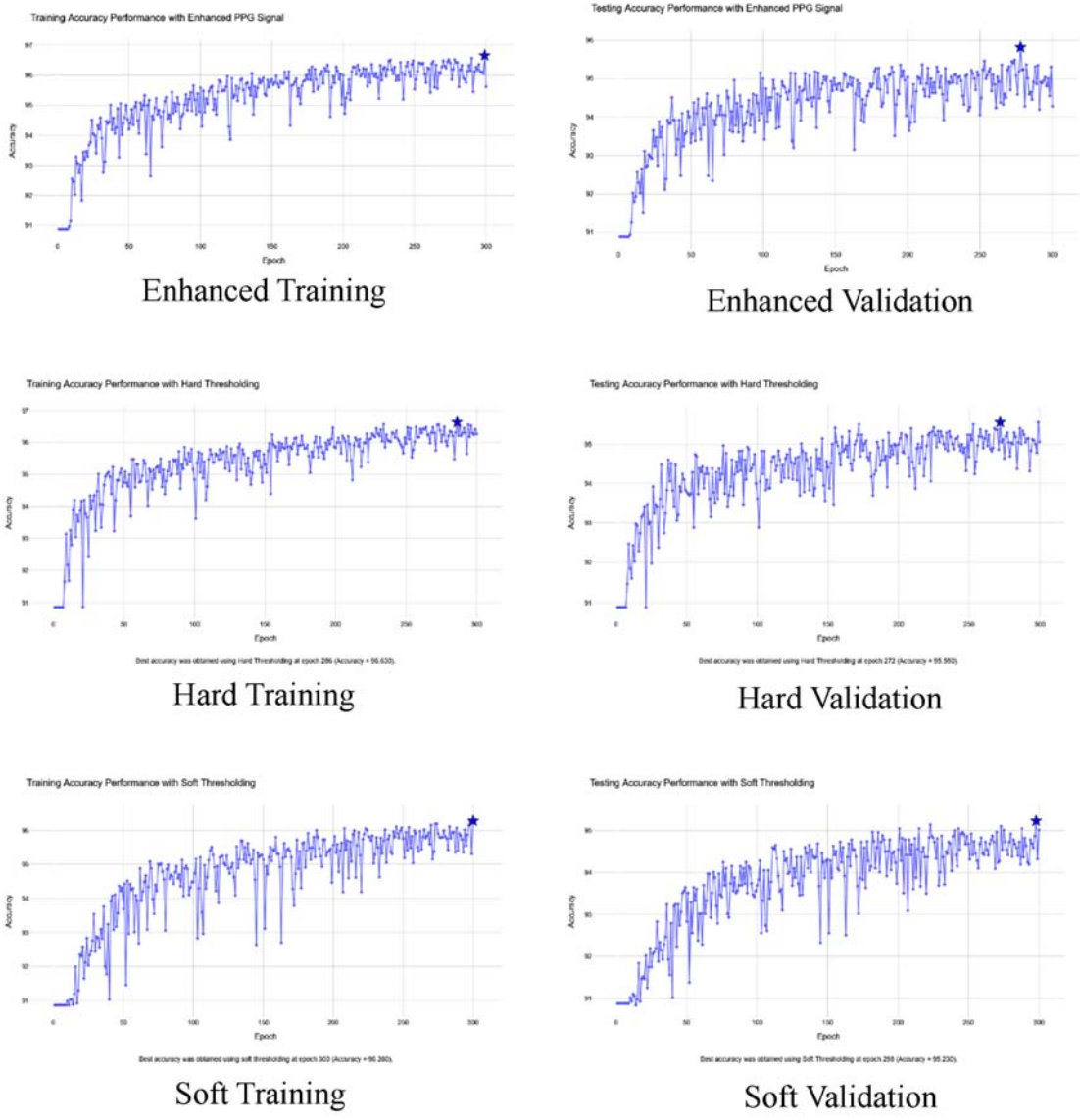

Figure 5: Comparison of training and validation accuracy using Enhanced, Hard, and Soft Thresholding. Each plot includes the best accuracy point for the model.

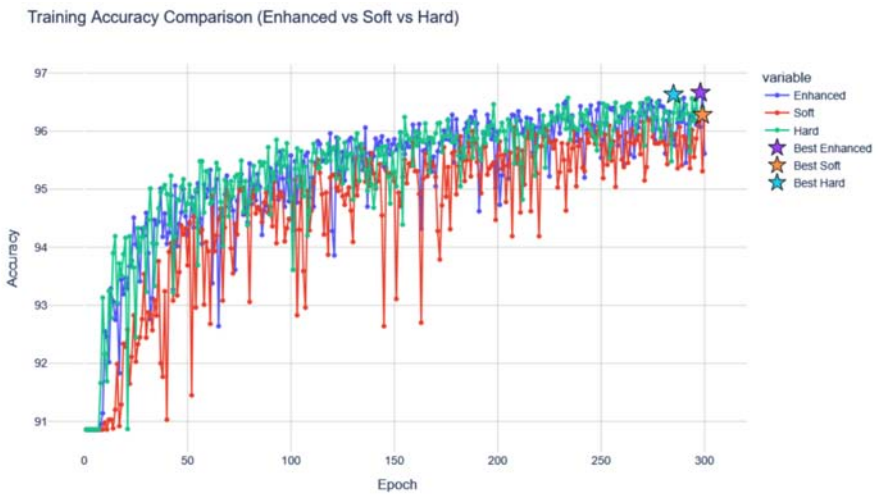

(a) Training Accuracy Comparison of Thresholding Methods

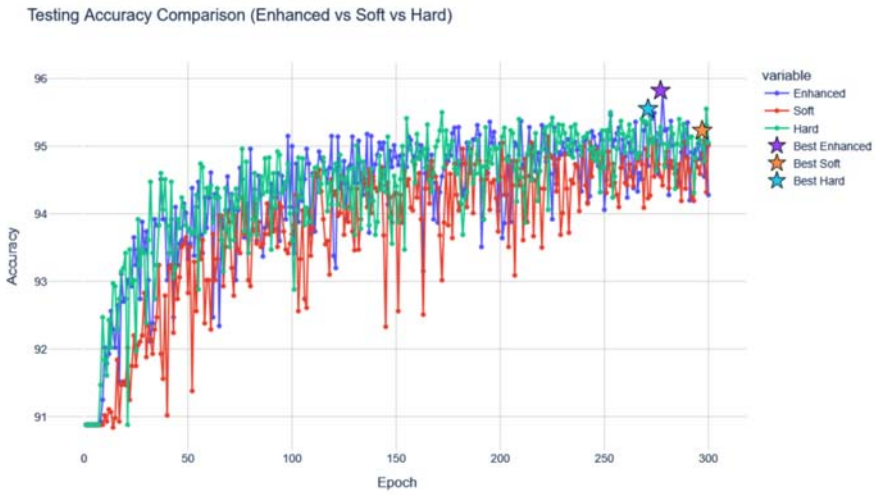

(b) Validation Accuracy Comparison of Thresholding Methods

Figure 6: Comparison of Training and Validation Accuracy Across Thresholding Methods Over Epochs.

approach achieved the highest validation accuracy at epoch 278 with 95.820%, followed by Hard Thresholding at epoch 272 with 95.550%, and Soft Thresholding at epoch 298 with 95.230%. These findings indicate that the enhanced approach provided a marginally better denoising capability and overall generalization performance compared to the other two thresholding techniques.

The heatmaps of training and testing accuracy and F1-score, shown in Figure **7**, further reinforce these findings by showing that the enhanced approach maintains higher accuracy levels and greater stability throughout the training process, while the Soft Thresholding method demonstrates more fluctuations and relatively lower performance ranges. These results align with the effectiveness of thresholding preprocessing techniques, including soft and hard thresholding, in enhancing model performance for non-invasive PPG data classification. The enhanced approach, in particular, appears to provide a more robust denoising capability, which contributes to its consistently better accuracy and F1-score outcomes on unseen data, supporting its suitability for BP dynamics classification in PPG signals.

From a physiological perspective, the performance of the enhanced approach can be further explained by its adaptability in processing photoplethysmogram (PPG) signals. PPG signals, being non-invasive in

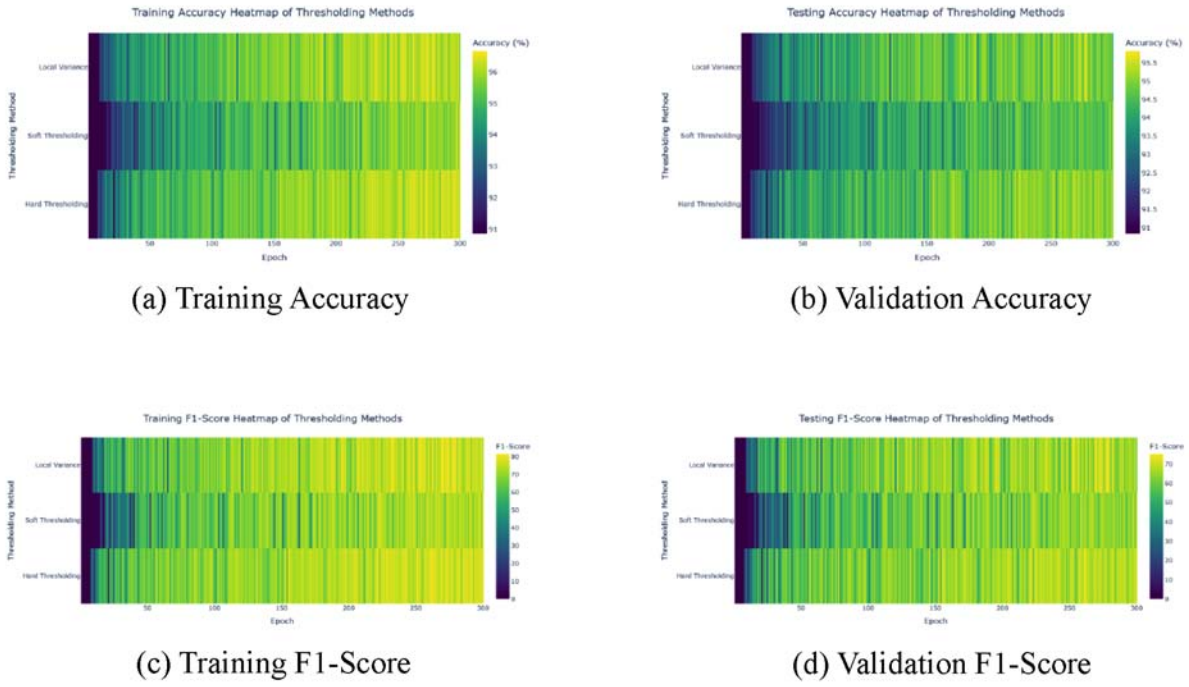

Figure 7: Heatmap Comparison of Accuracy and F1-Score Across Thresholding Methods and Epochs.

nature, are highly sensitive to motion artifacts, illumination changes, and peripheral noise. In contrast, the ART signal, obtained through invasive measurement, represents the true hemodynamic waveform with minimal distortion. Therefore, the ability of the preprocessing method to preserve essential morphological information from the PPG signal while effectively suppressing noise is critical for accurate estimation of the corresponding arterial characteristics. The enhanced approach adaptively processes the signal characteristics at different segments of the PPG waveform, enabling a better distinction between physiological variations and noise components. This adaptive behavior supports improved preservation of key temporal and amplitude features, such as systolic peaks, dicrotic notches, and diastolic slopes, which are essential for representing cardiovascular dynamics. Consequently, the enhanced preprocessing provides a more informative and stable input representation for the learning model, resulting in improved accuracy and generalization performance compared to both Hard and Soft Thresholding methods. In contrast, conventional thresholding approaches rely on more uniform processing strategies that may not fully capture local signal variations, potentially leading to either excessive smoothing or insufficient noise suppression. Such limitations can reduce their ability to retain subtle morphological features that are critical for accurate interpretation of non-invasive PPG signals.

A detailed quantitative comparison of performance metrics across various training epochs is presented in Table **3**. The results further confirm that the enhanced approach consistently yields the highest values across all evaluation metrics, including training and validation accuracy, precision, recall, and F1-score, emphasizing its robustness in modeling the physiological relationship between PPG and ART signals.

5. CONCLUSIONS

The results demonstrate that the application of signal enhancement in the preprocessing stage improves classification performance by effectively reducing noise in raw PPG signals, thereby enhancing both the quality and stability of the input data. This preprocessing step contributes to more accurate and robust estimation of BP dynamics from non-invasive PPG measurements. Among the evaluated approaches, the enhanced method shows a marginal but consistent improvement over conventional thresholding strategies, while maintaining stable learning behavior across training epochs. This improvement is associated with its ability to preserve key morphological features of the PPG waveform, which are essential for reliable representation of cardiovascular dynamics. These findings indicate that the enhanced preprocessing approach provides a more informative and stable input representation for the classification model.

Table 3: Comparison of Model Performance Across Epochs for Different Thresholding Methods

Threshold Type	Epoch	Train Acc (%)	Validation Acc (%)	Precision	Recall	F1-Score
Enhanced	10	92.55	92.02	77.49	26.05	39.00
	20	93.47	92.74	87.34	33.37	48.29
	50	94.20	93.33	95.11	38.59	54.90
	75	95.13	94.68	82.95	58.38	68.53
	100	95.58	95.00	78.42	70.20	74.08
	150	95.86	94.84	87.12	60.93	71.71
	175	95.91	94.78	88.63	62.38	73.22
	200	95.99	95.04	88.09	63.83	74.03
	250	95.54	94.06	95.55	53.49	68.59
	275	96.41	95.08	87.00	69.85	77.48
	299	**96.66**	**95.31**	**86.11**	**74.75**	**80.03**
Hard	10	92.16	91.84	95.28	15.01	25.94
	20	94.16	93.42	73.89	55.83	63.60
	50	94.75	93.78	88.81	48.44	62.69
	75	95.06	94.24	92.01	50.19	64.95
	100	94.84	95.00	91.39	47.69	62.67
	150	95.30	93.61	91.77	53.00	67.19
	175	94.89	94.41	84.24	65.14	73.47
	200	95.83	94.99	83.75	65.02	73.21
	250	95.96	94.68	90.46	61.86	73.47
	275	96.02	94.64	87.61	65.07	74.67
	286	**96.63**	**95.40**	**82.39**	**78.79**	**80.55**
Soft	10	90.98	91.02	100.00	1.36	2.69
	20	92.29	91.47	64.65	34.49	44.98
	50	93.69	92.83	92.81	33.62	49.36
	75	95.01	93.42	84.79	55.33	66.97
	100	94.48	93.70	77.08	56.33	65.09
	150	95.27	94.31	74.34	73.32	73.82
	175	94.87	93.83	71.17	73.12	72.13
	200	95.57	94.55	86.48	60.75	71.37
	250	95.76	94.68	83.57	65.99	73.75
	275	95.90	95.01	86.90	63.88	73.63
	300	**96.28**	**95.01**	**80.10**	**78.50**	**79.29**

This study further suggests that PPG signals, when properly processed and enhanced, have the potential to be utilized independently for BP classification tasks without relying on direct arterial pressure parameters such as SBP, DBP, or MBP. However, clinical validation remains necessary to confirm their physiological reliability and diagnostic accuracy. Future research may explore advanced deep learning frameworks that integrate signal enhancement with temporal modeling techniques to further improve classification performance. With ongoing technological developments, the use of PPG signals for direct BP classification presents promising opportunities, although further investigation is required to ensure its practical applicability in clinical environments.

ACKNOWLEDGEMENTS

The authors thank the Indonesia Endowment Fund for Education (LPDP) and the Ministry of Religious Affairs of the Republic of Indonesia (Kemenag) through the Beasiswa Indonesia Bangkit program for their financial support in facilitating this doctoral research.

FUNDING

This research received no specific grant from any funding agency in the public, commercial, or not-for-profit sectors.

DATA AVAILABILITY

The data used in this study are publicly available from the VitalDB database. The dataset can be accessed through PhysioNet and Scientific Data, as described in [15, 16].

DECLARATIONS

The authors declared no potential conflicts of interest with respect to the research, authorship and/or publication of this article.

REFERENCES

[1] Rastegar S, Gholam Hosseini H, Lowe A. Non-invasive continuous blood pressure monitoring systems: current and proposed technology issues and challenges. Physical and Engineering Sciences in Medicine 2019; 43(1): 11-28. https://doi.org/10.1007/s13246-019-00813-x

[2] Allen J. Photoplethysmography and its application in clinical physiological measurement. Physiological Measurement 2007; 28(3): 1-39. https://doi.org/10.1088/0967-3334/28/3/r01

[3] Asad A, Sarwar M, Aslam M, Akpokodje E, Jilani SF. Multiscalefusion-net and resrnn-net: Proposed deep learning architectures for accurate and interpretable pregnancy risk prediction. Applied Sciences 2025; 15(11): 6152. https://doi.org/10.3390/app15116152

[4] Batool I. Real-time health monitoring using 5g networks: Deep learning-based architecture for remote patient care. Journal of Medical Internet Research 2025; 6: 70906-70906. https://doi.org/10.2196/70906

[5] Oleiwi ZC, AlShemmary EN, Al-Augby S. Developing hybrid cnn-gru arrhythmia prediction models using fast fourier transform on imbalanced ecg datasets. Mathematical Modelling of Engineering Problems 2024; 11(2): 413-429. https://doi.org/10.18280/mmep.110213

[6] Donoho D, Johnstone IM. Adapting to unknown smoothness via wavelet shrinkage. Journal of the American Statistical Association 1995; 90(432): 1200-1224. https://doi.org/10.1080/01621459.1995.10476626

[7] Donoho D. De-noising by soft-thresholding. IEEE Transactions on Information Theory 1995; 41(3): 613-627. https://doi.org/10.1109/18.382009

[8] Donoho D, Johnstone IM. Minimax estimation via wavelet shrinkage. The Annals of Statistics 1998; 26(3). https://doi.org/10.1214/aos/1024691081

[9] Alzubaidi L, Zhang J, Humaidi AJ, Al-Dujaili A, Duan Y, Al-Shamma O, Santamaria J, Fadhel MA, Al-Amidie M, Farhan L. Review of deep learning: concepts, cnn architectures, challenges, applications, future directions. Journal of Big Data 2021; 8(1). https://doi.org/10.1186/s40537-021-00444-8

[10] Alqudah A, Moussavi Z. A review of deep learning for biomedical signals: Current applications, advancements, future prospects, interpretation, and challenges. Computers, Materials & Continua 2025; 83(3): 4567-4592 https://doi.org/10.32604/cmc.2025.063643

[11] Mienye ID, Swart TG, Obaido G, Jordan M, Ilono P. Deep convolutional neural networks in medical image analysis: A review. Information 2025; 16(3): 195. https://doi.org/10.3390/info16030195

[12] Lee J, Mukhanov L, Molahosseini AS, Minhas U, Hua Y, Rincon J, Dichev K, Hong C-H, Vandierendonck H. Resource-efficient convolutional networks: A survey on model-, arithmetic-, and implementation-level techniques. ACM Computing Surveys 2023; 55(13s): 1-36. https://doi.org/10.1145/3587095

[13] Chen S, Ji Z, Wu H, Xu Y. A non-invasive continuous blood pressure estimation approach based on machine learning. Sensors 2019; 19(11): 2585. https://doi.org/10.3390/s19112585

[14] Hong J, Jin W, Nandi M, Alastruey J. Real-time classification of blood pressure changes using photoplethysmography and deep learning. Biomedical Signal Processing and Control 2026; 112: 108380. https://doi.org/10.1016/j.bspc.2025.108380

[15] Lee H-C, Park Y, Yoon SB, Yang SM, Park D, Jung C-W. Vitaldb, a high-fidelity multi-parameter vital signs database in surgical patients. Scientific Data 2022; 9(1). https://doi.org/10.1038/s41597-022-01411-5

[16] Lee H-C, Jung C-W. VitalDB, a high-fidelity multi-parameter vital signs database in surgical patients. Physio Net 2022. https://doi.org/10.13026/W758-NW21

[17] Mallat S. A Wavelet Tour of Signal Processing, 2nd edn. Academic Press, San Diego 1999.

[18] Muralidharan A, Mahfuz S. Human activity recognition using hybrid cnn-rnn architecture. Procedia Computer Science 2025; 257: 336-343 https://doi.org/10.1016/j.procs.2025.03.045

[19] Nurtiyasari D, Rosadi D, Abdurakhman A, Sumardi S. Performance evaluation for Indonesia sharia stocks price prediction integrating wavelet and hybrid approaches. Industrial Engineering & Management Systems 2025; 24(2): 211-224. https://doi.org/10.7232/iems.2025.24.2.211

Received on 12-03-2026 Accepted on 08-04-2026 Published on 28-04-2026

https://doi.org/10.6000/1929-6029.2026.15.15